Environmental Pollution 239 (2018) 648–660

Contents lists available at ScienceDirect

Environmental Pollution

journal homepage: www.elsevier.com/locate/envpol

Current and future hot-spots and hot-moments of nitrous oxide emission in a cold climate river basin☆

Narayan Kumar Shrestha, Junye Wang*

Athabasca River Basin Research Institute (ARBRI), Athabasca University, 1 University Drive, Athabasca, Alberta, T9S 3A3, Canada

ARTICLE INFO

Article history:
Received 11 February 2018
Received in revised form
15 April 2018
Accepted 15 April 2018
Available online 27 April 2018

Keywords:
Cold climate river basin
N_2O hot-spots and hot-moments
ARB
SWAT

ABSTRACT

An ecosystem in a cold climate river basin is vulnerable to the effects of climate change affecting permafrost thaw and glacier retreat. We currently lack sufficient data and information if and how hydrological processes such as glacier retreat, snowmelt and freezing-thawing affect sediment and nutrient runoff and transport, as well as N_2O emissions in cold climate river basins. As such, we have implemented well-established, semi-empirical equations of nitrification and denitrification within the Soil and Water Assessment Tool (SWAT), which correlate the emissions with water, sediment and nutrients. We have tested this implementation to simulate emission dynamics at three sites on the Canadian prairies. We then regionalized the optimized parameters to a SWAT model of the Athabasca River Basin (ARB), Canada, calibrated and validated for streamflow, sediment and water quality. In the base period (1990–2005), agricultural areas (2662 gN/ha/yr) constituted emission hot-spots. The spring season in agricultural areas and summer season in forest areas, constituted emission hot-moments. We found that warmer conditions (+13% to +106%) would have a greater influence on emissions than wetter conditions (−19% to +13%), and that the combined effect of wetter and warmer conditions would be more offsetting than synergetic. Our results imply that the spatiotemporal variability of N_2O emissions will depend strongly on soil water changes caused by permafrost thaw. Early snow freshet leads to spatial variability of soil erosion and nutrient runoff, as well as increases of emissions in winter and decreases in spring. Our simulations suggest crop residue management may reduce emissions by 34%, but with the mixed results reported in the literature and the soil and hydrology problems associated with stover removal more research is necessary. This modelling tool can be used to refine bottom-up emission estimations at river basin scale, test plausible management scenarios, and assess climate change impacts including climate feedback.

1. Introduction

Cold climate regions, such as the Athabasca River Basin (ARB) in western Canada, are some of the most sensitive eco-regions in the world and the slightest of the changes in climate would lead to significant alterations in snow-melt dominated hydrologic, sediment and nutrient transport processes, freeze-thaw cycles, and soil water and temperature (Eum et al., 2017; IPCC, 2007, 2014; Kurylyk et al., 2014). There is much evidence showing an accelerated release of GHGs (Helbig et al., 2017; Schuur et al., 2015), changes in the composition of bacterial communities (Rofner et al., 2017), and the mobilization and export of dissolved organic carbon (Olefeldt and Roulet, 2014; Tesi et al., 2016) due to thawing of permafrost in these regions. Changes to these environmental variables could also significantly affect N_2O emissions (Butterbach-Bahl et al., 2013; Voigt et al., 2017). To date, contrasting results are presented on how much the inevitable effects of climate change would influence N_2O emissions (Abalos et al., 2016; Del Grosso and Parton, 2012; Iqbal et al., 2018; Kanter et al., 2016). Understanding nutrient cycle responses to warming-induced environmental changes, such as permafrost thaw and glacier retreat, is critical to evaluating their influences on soil biogeochemical cycles and N_2O emissions in a cold climate river basin as the large-scale, cold climate river basin is a natural water system boundary and represents a complex organized system, such as an ecosystem or a society, as a macrocosm region.

Site-based measurements are able to capture the N_2O dynamics

☆ This paper has been recommended for acceptance by Dr. Jorg Rinklebe.

* Corresponding author.
E-mail address: junyew@athabascau.ca (J. Wang).

https://doi.org/10.1016/j.envpol.2018.04.068
0269-7491/

quite well at a localized scale. However, these measurements are cumbersome and continuous emission measurements are practically impossible unless an automatic and online system is available (Liao et al., 2013; Smith and Dobbie, 2001). Furthermore, these point measurements might include considerable uncertainties as the drivers of N_2O flux vary both spatially and temporally (Butterbach-Bahl et al., 2013; Raich and Tufekciogul, 2000). Moreover, could not be up-scaled due to spatial heterogeneity at the river basin or regional scale. Hence, there is also a growing realization of the need to monitor N_2O emissions hot-spots and hot-moments in river basins (Groffman et al., 2009). Recent studies suggest that much attention has been paid in capturing these emission hot-moments, such as during freeze-thaw cycles, as they seem to dominate the annual emission budget of cold climate river basins (Flechard et al., 2005; McClain et al., 2003; Pelster et al., 2013). However, identification of emission hot-spots, which might be more challenging and costly, is equally important (Groffman et al., 2009). Usually, N_2O estimations at the river basin scale have been carried out using the IPCC inventory with “emission factors” (IPCC, 2006). However, such simplistic methods are often inaccurate as they can't incorporate variations of land management practices (e.g. tillage operation) and the dynamics of environmental variables (e.g. soil moisture and temperature) at a finer temporal scale. Furthermore, such “top-down inventories” have shown to significantly underestimate the level of emissions (Eric, 2014; Turner et al., 2015).

As a result, process-based modelling tools have become an attractive alternative (Li et al., 1992; Schmid et al., 2001). Such modelling tools are not only helpful in identifying emissions hot-spots and hot-moments, but are also useful in assessing the effectiveness of different management options for evaluating the impacts of climate and land-use changes (Butterbach-Bahl et al., 2013), and for climate feedback (Schuur et al., 2015). A process based model should be able to dynamically simulate the main drivers of N_2O emissions, including interactions between soil, water, vegetation, and nutrients, and should also be flexible enough to incorporate finer spatial and temporal resolution datasets, which are becoming more available through advancements in remote sensing technology (Groffman et al., 2009; McClain et al., 2003). Many such models have been developed to simulate N_2O from soils such as JULES (Best et al., 2011; Clark et al., 2011), DNDC (Li et al., 1992), DAYCENT (Del Grosso et al., 2001), CENTURY (Parton, 1996), Roth-C (Coleman and Jenkinson, 1996), etc. However, these models primarily use the vertical transfer of hydrological and substrate fluxes and lack consideration of the lateral transport of water and nutrients (Groffman et al., 2009). More importantly, typical water cycle regions are river basins acting as natural water system boundaries. Therefore, models should be able to simulate the “lateral flow and distribution of water, nitrogen and carbon within landscapes” (Groffman et al., 2009), stream flows, and sediment and nutrients runoff in river networks. Moreover, cold climate regions consist of agriculture, forests, wetland, peatland, permafrost and glacier regions, which are the most efficient terrestrial carbon stores on Earth (AWC, 2014). Such cold climate regions service multiple other ecosystem functions, such as climate regulation, water filtration, and biodiversity (Black, 1997). In such regions, the N_2O emissions during freeze-thaw conditions need to be accurately represented (Butterbach-Bahl et al., 2013; Flechard et al., 2005; Groffman et al., 2009; Kravchenko et al., 2017; McClain et al., 2003; Pelster et al., 2013). Furthermore, a model should represent special processes related to cold climate regions, such as the ability to simulate areal snow distribution, freeze-thaw cycles, stream flow and snow melt processes comprehensively. Whereas, N_2O emissions have been monitored or simulated globally, we lack sufficient data on how, or if, hydrological processes, such as flooding, drought, erosion and sediment transport, permafrost thaw and snowmelt, affect N_2O emissions in a cold climate river basin since the transport of water and nutrients are one of the most important components in the water and nutrient cycle.

In this context, a widely used process-based hydrological model – the Soil and Water Assessment Tool (SWAT) (Arnold et al., 1998) has been tested for short and long-term simulations of hydrological, sediment and water quality processes all around the world, irrespective of climate or the shape and size of river basins (Abbaspour et al., 2015; Arnold et al., 2012; Kannan et al., 2006; Leta et al., 2014; Ligaray et al., 2017; Meng et al., 2018; Shrestha et al., 2013, 2014). This tool possesses all the attributes required, as pointed out by Groffman et al. (2009), for the simulation of N_2O hot-spots and hot-moments at a regional scale. While the model considers both nitrification and denitrification processes in its nitrogen-cycling algorithm (Neitsch et al., 2011), it does not explicitly estimate N_2O emissions, which could introduce uncertainty into the estimation of N and C stocks.

With this in mind, we incorporated the well-established semi-empirical equations of nitrification and denitrification processes (Parton et al., 1996, 2001) into the SWAT model, to explicitly estimate N_2O emissions from both nitrification and denitrification. These equations can be considered conceptual as they relate soil carbon, ammonia, nitrate, moisture, temperature, and pH to N_2O emissions (Butterbach-Bahl et al., 2013). The SWAT model is then tested to simulate short-term, site-based N_2O measurements from three sites (cropped, shelterbelt and grassland) in the Canadian prairies. In order to estimate N_2O emissions in the ARB: (a) a comprehensive SWAT model of the ARB was built-up using high-resolution spatial and meteorological data sets, considering both point and non-point pollution sources, and defining appropriate crop, pasture, grassland, and forest related management practices; (b) multi-variable (streamflow, sediment and water quality), multi-site (35 streamflow, 5 sediment and 10 water quality monitoring stations), and multi-objective sensitivity, calibration and validation, and uncertainty analysis has been carried out with special consideration of snow-melt processes; (c) optimized land-use type N_2O related parameters were regionalized to the ARB. Moreover, we quantified the N_2O emissions in different land-use types, seasons, and regions in the ARB to identify the N_2O hot-spots and hot-moments. Next, we assessed climate change impacts on the N_2O dynamics of the ARB using future climate data from bias-corrected spatial disaggregated high-resolution datasets from the top three Coupled Model Intercomparison Project (CMIP5) Global Circulation Models (GCMs) for the Western North America region. Finally, different fertilizer, crop residue management, and grazing scenarios were tested to evaluate the effectiveness of possible N_2O abatement methods. To our knowledge, this is the first study of its kind in which SWAT was used to estimate current and future N_2O emissions in a large cold climate region watershed and to understand how the hydrological processes affect N_2O emissions. We believe that this modelling tool can be used in other regions to refine the bottom-up emission inventories, and that results of this study can be translated into a process for managing the N_2O emissions of the ARB.

2. Material and methods

2.1. The study area

The Athabasca River Basin (ARB) runs upward in central Alberta, Canada and provides a dependable water supply source for major urban centers (Jasper, Hinton, Whitecourt, Athabasca, and Fort McMurray) and its major industries (agriculture, forestry, pulp and

paper, coal, oil and oil-sands mining), thereby contributing significantly to the provincial economy (AWC, 2013). The river, originating in the Canadian Rocky Mountains, flows to the North-East and drains a total area of about 160,000 km^2 into the Lake Athabasca (Fig. 1).

2.2. The simulator

The Soil and Water Assessment Tool (SWAT) is a physical-based hydrologic simulator capable of continuous, long-term simulation of a variety of processes such as hydrology, sediment, nutrients, metals, bacteria, etc. (Arnold et al., 1998). We refer Neitsch et al. (2011) for details of the equations that SWAT uses for each processes, however, some governing equations for hydrology, snow accumulation, distribution and melting, erosion and sediment transport and water quality processes are presented in Section S1. While the simulator accounts for both nitrification and denitrification processes in its nitrogen cycling routine, it does not explicitly estimate the production of N_2O. For this, Yang et al. (2017) migrated the DAYCENT model's N_2O emission module to the SWAT and Wagena et al. (2017) have incorporated the semi-empirical equations of Parton et al. (1996) with some minor changes. In our implementation, we preferred to adopt the original formulation of Parton et al. (2001); Parton et al. (1996) as this formulation has been widely tested around the world. Hence, our implementation is similar to that of Wagena et al. (2017) with some changes, which we will illustrate next.

These semi-empirical equations, in general, calculate the potential N_2O emission rate based on substrate concentrations. This potential rate is then subjected to several reduction factors (Butterbach-Bahl et al., 2013). For the N_2O emission from denitrification, the total emissions are partitioned between N_2 and N_2O, using a ratio method.

$$DENIT_{total} = \min[F_{denit}(NO3), F_{denit}(C)]*F_{denit}(WFPS)*F_{denit}(SOLT) \quad (1)$$

$$Ratio_{\mathrm{N2:N2O}} = \min[F_{ratio}(\mathrm{NO3}), F_{ratio}(\mathrm{C})]*F_{ratio}(\mathrm{WFPS}) \quad (2)$$

$$F_{\mathrm{N2O,denit}} = \frac{DENIT_{total}}{(1 + Ratio_{\mathrm{N2:N2O}})} \quad (3)$$

Where, $DENIT_{total}$: is the total emissions from denitrification (g/ha/day), $Ratio_{N2:N2O}$: proportion of N_2 and N_2O emissions during denitrification (-), $F_{N2O,denit}$: N_2O emissions from denitrification (g/ha/day), $F_{denit}(NO3)$ & $F_{denit}(C)$: denitrification rate for a given soil nitrate and carbon level, respectively (gN/ha/day), $F_{denit}(WFPS)$ &$F_{denit}(SOLT)$: soil moisture and temperature reduction factors for the total denitrification rate, respectively (-), and $F_{ratio}(WFPS)$: the soil moisture reduction factor for the ratio (-). Refer to supplementary section S2 for details of these equations.

While Wagena et al. (2017) considered pH reduction factors for the calculation of both total denitrification rate and the ratio, we preferred the Parton et al. (1996) original formulation, which does not include the pH reduction factors as pH is not a dynamics variable in the SWAT model.

Next, for the total N_2O emissions from nitrification, a nitrification rate based on net nitrogen mineralization and soil NH_4 level is first calculated and subjected to reduction factors.

$$F_{\mathrm{N20,nit}} = K_2*F_{\mathrm{N03,nit}} \quad (4)$$

$$F_{\mathrm{NO3,nit}} = Net_{\min}*K_1 + K_{\max}*\mathrm{NH4}*F_{nit}(SOLT)*F_{nit}(WFPS)*F_{nit}(pH) \quad (5)$$

where, $F_{N20,nit}$: N_2O emissions from nitrification (g/ha/day), K_2 (-): fraction representing the nitrified nitrogen that is lost as N_2O,

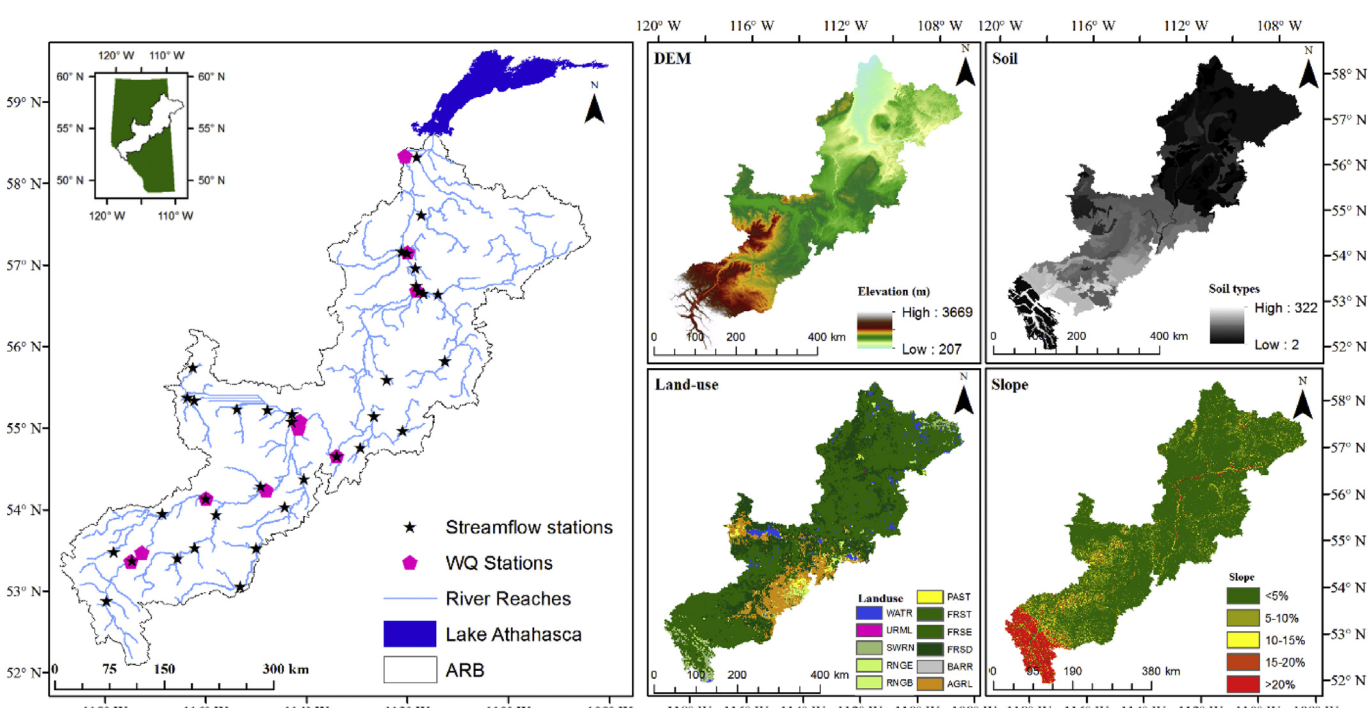

Fig. 1. Location of the Athabasca River Basin (ARB) in Alberta, Canada with the river network, Lake Athabasca, and its streamflow and water quality monitoring stations (left panel); the digital elevation model, soil, land-use and soil map of the ARB (right panels).

$F_{NO3,nit}$ (gN/ha/day): nitrification rate, Net_{min} (gN/ha/day): net nitrogen mineralization, K_1 (-): nitrified fraction of the net nitrogen mineralization, K_{max} (1/day): maximum fraction of the NH_4 that can be nitrified, NH_4 (gN/ha/day): ammonia level in the soil layer; F_{nit}(SOLT), F_{nit}(WFPS), and F_{nit}(pH) are soil temperature, moisture and pH reduction factors, respectively.

In their formulation, Wagena et al. (2017) calculated nitrogen removed from the ammonia pool by nitrification, as in the original SWAT model (Neitsch et al., 2011), which is then subjected to pH, soil moisture and temperature reduction factors. In our implementation, we again preferred the Parton et al. (2001) original formulation, thereby keeping consistency in sources of equations used. Further studies are indeed needed to verify robustness of these different formulations.

Finally, the N_2O emissions from both nitrification and denitrification, estimated at Hydrological Response Unit (HRU) spatial scale, are summed up to obtain the total emissions. The total can then be aggregated into the sub-basin and watershed spatial scale.

2.3. Model inputs, build-up, sensitivity, calibration and validation, and uncertainty analysis

We used a 90m × 90m Digital Elevation Model - DEM (Jarvis et al., 2008), a 1 km × 1 km land-use, and an 1:1 million scale soil map (SLC, 2010) to build-up the SWAT model of the ARB (Fig. 1). A threshold drainage area of 200 km^2 for sub-basin delineation and threshold percentages of 10%, 5% and 10% for land-use, soil, and slope, respectively, resulted in a total of 131 sub-basins and 1370 HRUs. Daily precipitation, and maximum and minimum temperatures data (GoC, 2016) and daily relative humidity, solar radiation and wind speed data (CFSR, 2016) were also used. Moreover, point source pollution from four waste water treatment plants were also considered. Appropriate management operations such as plantation and harvesting (AGRI-FACTS, 2013), fertilizer application (AGRI-FACTS, 2004), grazing, trampling and manure deposition (AGRI-FACTS, 1998), were considered for each land-use type for non-point sources of pollution.

We considered streamflow (Table S1), sediment (Table S2), water quality (Table S3), and N_2O (Table S4) related parameters for sensitivity analysis using a wider range of parameter values in the SWAT-CUP (Abbaspour et al., 2004). The model was run for a period of 34 years (1980–2013), with 3 years (1980–1982) of warming-up, 16 years (1990–2005) of calibration and the remaining years as validation period. The warming-up period was required to stabilize various hydrological (e.g. soil moisture), water quality (e.g. carbon pools) related variables, among others, and the calibration period included almost equal numbers of dry and wet years. The simulation results were calibrated and validated using 35 streamflow, 5 sediment and 10 water quality monitoring stations (Fig. 1). Model performance was evaluated using several goodness-of-fit statistics: the percentage of bias (PBIAS), the Nash-Sutcliffe Efficiency (NSE) (Nash and Sutcliffe, 1970), the ratio of root mean squared error to standard deviation (RSR), coefficient of determination (R^2) and mean absolute error (MAE). We also used the p- and r-statistics (Abbaspour et al., 2004) to optimize a 95% predictive uncertainty band. Simulated results are assigned with one of the four qualitative ratings (very good, good, satisfactory and unsatisfactory) as per the range of values of the chosen goodness-of-fit statistics, as suggested by Moriasi et al. (2007); Moriasi et al. (2015), see Table S5.

We refer to Shrestha et al. (2017); Shrestha and Wang (2017) for streamflow, Shrestha and Wang (2018) for erosion and sediment transport, and Shrestha and Wang (Accepted) for water quality related results. However, we have presented goodness-of-fit statistics of the simulated streamflow (Table S6), sediment load (Table S7), and water quality variables (Table S8).

As there are no N_2O measurements inside the ARB, we have calibrated and validated the N_2O simulation against observations made on different land-use types in similar cold climatic regions and regionalized them to the ARB. As such, we used 2-years of N_2O measurements of Amadi et al. (2016) on a cropped and a shelterbelt site in Outlook, Saskatchewan, Canada (refer Table S9 for the site characteristics), to calibrate and validate N_2O related parameters of respective land-use types. The emissions were measured using rectangular gas chambers from spring thaw (April 29, 2013) to soil freeze up (October 9, 2014), and at the same time soil moisture and temperature were also measured besides the gas chambers. Readers can refer to Amadi et al. (2016) for further details of the measurements. We used year 2013 as a calibration period and year 2014 as a validation period, with 2 years of warming up period. To this end, the initial conditions (e.g. soil NO_3 level, Table S9) were imposed based on or calculated from (Amadi et al., 2016). Furthermore, we used 3 years of N_2O measurements from Gao et al. (2018) on a heavily grazed grassland site in Stavely, Alberta, Canada (refer Table S9 for the site characteristics), to calibrate and validate N_2O related parameters of the land-use type. The emission were measured using gas chambers in a weekly basis (15 weeks in 2013: May 28 to September 17; 18 weeks in 2014: May 15 to October 22; and 19 weeks in 2015: May 13 to October 7), and at the same time soil moisture at location adjacent to the gas chambers were also measured. We refer Gao et al. (2018) for further details of the measurements. For this, we considered years 2013-14 as the calibration period and year 2015 as the validation period, with 3 years of warming up period. As such, the initial conditions (e.g. soil NO_3 level, Table S9) were imposed based on or calculated from Gao et al. (2018).

For both cases, as already depicted, we used SWAT-CUP for model calibration and validation. As such, all N_2O related parameters (Table S4) and other related parameters which affects the environmental variables (e.g. soil temperature, moisture, etc.) are given a wider range (maximum and minimum value) which lead to the multi-variable calibration and validation scheme in which the parameters related to environmental variables and N_2O would be optimized simultaneously. The SWAT-CUP is then run 100 times with the NSE, as the objective function. The program would return an optimized set of parameter values and would also recommend a new range of parameter values. We then evaluated the goodness-of-fit statistics for the optimized set of parameter and evaluated the p- and r-stat. If needed, SWAT-CUP would be run for another 100 times with a carefully selected new parameter range until we got near to sought values (e.g. p-stat > 0.7 and r-stat <1.5). In doing so, a compromised solution would have to be accepted in some cases. For example, a higher value of p-stat can be achieved with an increased r-stat and vice-versa.

2.4. Future climatic data

For the Western North America region (Giorgi and Bi, 2005), Murdock et al. (2013) assessed the accuracy of 26 CMIP5 GCMs and ranked them. Using various downscaling methods, Murdock et al. (2013) prepared high resolution bias-corrected future climate data at 0.0833° (~10 km) spatial resolution. We used the top three ranked GCMs and their Bias-Correction/Spatial Disaggregation (BCSD) products. To reduce different sources of uncertainties in future climatic projections (Hawkins and Sutton, 2009), we considered two IPCC AR5 (IPCC, 2014) emission scenarios (RCP 4.5 and 8.5) and two future periods (mid-: 2021–2060 and end-century: 2061–2100), making a total of 12 combinations for a month. We calculated basin averaged changes in monthly precipitation (%) and mean air temperature (°C), as compared to the base

period (1990–2005) and plotted them (Figure S1). We encapsulated all these data points in a rectangular envelop, an approach advocated by Lutz et al. (2016), to select four representative future climatic scenarios; namely Drier-Colder, Drier-Warmer, Wetter-Colder and Wetter-Warmer. These scenarios were then applied to the calibrated and validated SWAT model of the ARB to assess their impacts on the N_2O dynamics.

2.5. Scenario analysis

Four management scenarios for agriculture land-use and one scenario each for pasture and grassland land-use types have been formulated and tested. For the agricultural land-use, we split single fertilizer applications in the base period into four applications with apportionment of 40% before seedling, 10% with seed, 25% during tillering (Zadoks Growth Stage 21–26) and 25% during stem elongation stage (Zadoks Growth stage 30–32) (AAF, 2017), as the first scenario (Sc-1, Table 1). For the Sc-2, we used the minimum amount of fertilizer as a single application, which is the lower limit of recommended dose in Alberta (AGRI-FACTS, 2004). Splitting this dose into four applications, as above, would form the Sc-3. The three remaining scenarios (Sc-4(a) to (c)) are related to crop residue harvest and management as recent researches have shown contrasting results as to what extent crop residue harvest would impact the emission (Baker et al., 2014; Campbell et al., 2014; Jin et al., 2014, 2017). As such, we arbitrarily fixed values of residue harvest index (HI_OVR) with the stover fraction removed (FRAC_HARVK) at 1% (Sc-4(a)), 75% (Sc-4(b)) and 99% (Sc-4(c)), to reflect the efficiency of residue crop management. One can indeed question the practical aspects of such a high stover removal rates (e.g. Sc-4(c)) as researches show economically optimal stover removal rate in the range of 30–50% for bio-energy use (Khanna and Paulson, 2016; Scarlat et al., 2010). However, some other studies have tested the effect of high (up to 75%) (Jin et al., 2014, 2017) to full (100%) (Baker et al., 2014) stover removal rates on the emission. However, the economic viability of such high rate of stover removal, and other benefits and pitfalls have to be further investigated. As for pasture, we used the minimum recommended dose of fertilizer (AGRI-FACTS, 1998) (Sc-5). Finally, for grassland, we aimed at restricting grazing to a light grazing intensity (Sc-6).

3. Results

3.1. Model validation based on short-term N_2O measurements at three isolated sites

At the agricultural site, the model has represented the dynamics of SOLT, WFPS and N_2O (Fig. 2a) quite well, which resulted in "very good" quality of model results in the calibration period. Simulated SOLT in the calibration period are in good agreement with observations with a low PBIAS (2.48%) and MAE (1.82 °C), and near optimal NSE (0.89), RSR (0.33) and R^2 (0.89). The 95% predictive uncertainty band captured 75% (p-value = 0.75) of its observations in a relatively thin band (r-stat = 0.84). However, model consistently underestimated SOLT in the validation period, resulting in slightly lower values of the goodness-of-fit statistics. While the model missed some WFPS observations, it tended to capture the variability of the observations. Furthermore, the 95% predictive uncertainty band encapsulated 71% of the observations within a thin band (r-stat = 0.55). All the statistics point to "very good" WFPS results in the calibration period, while a lower performance rating ("satisfactory") has been observed during the validation period. The N_2O simulation results are also of "very good" accuracy for both the calibration and validation periods.

Table 1
Tested management scenarios.

Land-use Types→		Agriculture land[a]			Pasture			Grassland	
Cases↓		N-Application	P-Application	Frequency and Timing	N-Application	P-Application	Frequency and Timing	Grazing	Manure
Base Case		100 lb N/ac[c]	35 lb P2O5/ac[d]	1 and Spring (April 1)	200 lb N/ac[e]	60 lb P2O5/ac[f]	4 and refer[e]	6 kg/ha/day[k]	5.5 kg/ha/day[k]
Scenarios	Sc-1	same as base	same as base	4 and see below[b]	–	–	–	–	–
	Sc-2	40 lb N/ac	20 lb P2O5/ac2	same as base	–	–	–	–	–
	Sc-3	same as Sc-2	same as Sc-2	same as Sc-1	–	–	–	–	–
	Sc-4(a)	same as base	same as base	same as base but different residue management[g]	–	–	–	–	–
	Sc-4(b)	same as base	same as base	same as base but different residue management[h]	–	–	–	–	–
	Sc-4(c)	same as base	same as base	same as base but different residue management[i]	–	–	–	–	–
	Sc-5	–	–	–	70 lb N/ac[j]	35 lb P2O5/ac[j]	4 and refer[e]	–	–
	Sc-6	–	–	–	–	–	–	2.4 kg/ha/day[l]	0.89 kg/ha/day[l]

[a] Spring Wheat or Barley.
[b] 40% in Spring (April 1), 10% at seedling (May 1), 25% at Tillering (June 15), 25% at Flowering/Stem Elongation.
[c] Economically optimal rate of N-application as per AGRI-FACTS (2013), range 40–130 lb N/ac.
[d] Average of the range of values (20–50 lbP2O5/ac) as per AGRI-FACTS (2004).
[e] Four applications for 2 cuttings, 60 lb N/ac in early spring, 50 lb N/ac in mid-June, 50 lb N/ac in mid-July, 40 lb N/ac mid-August. Range 70–110 ln N/ac without irrigation and 200lb N/ac with irrigation. Refer AGRI-FACTS (2005a,b).
[f] One application of 60 lb P2O5/ac in early spring. Range 70–110 ln N/ac and 35–45 lb P2O5/ac for without irrigation and 60 lb P2O5/ac with irrigation. Refer AGRI-FACTS (2005a,b).
[g] In base case, residue Harvest Index (HI_OVR) would vary between 0.25 (at worst water stressed condition) and 0.45 (optimal condition) as per water stress factor, so as the Stover Fraction Removed (FRAC_HARVK). Refer Arnold et al. (2011). In this scenario, values of HI_OVR and FRAC_HARVK are fixed at 1% (meaning 99% left in the field).
[h] Values of Harvest Index (HI_OVR) and Stover Fraction Removed (FRAC_HARVK) are fixed at 75% (meaning 25% left in the field).
[i] Values of Harvest Index (HI_OVR) and Stover Fraction Removed (FRAC_HARVK) are fixed at 99% (meaning only 1% left in the field).
[j] Minimum value of the range as specified in AGRI-FACTS (2005a,b).
[k] Values calculated considering 2 ac/cow, dry weight of biomass consumed = 11 kg/ha/day (5–16 lb/ac/day) and moisture content = 85%. Refer AGRI-FACTS (1998).
[l] As per Light Grazing (1.2 AMU/ha) intensity, as per Gao et al. (2018).

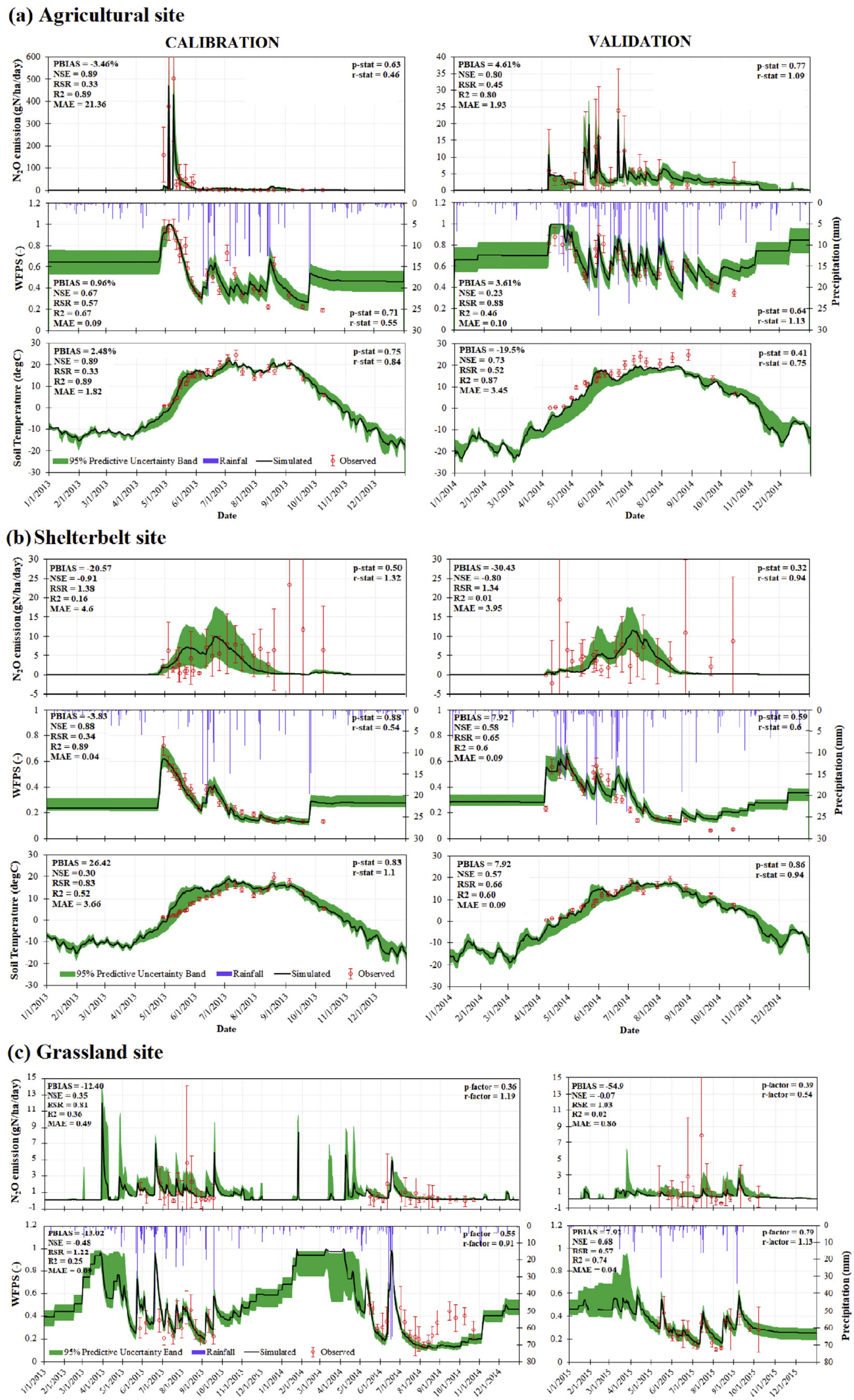

Fig. 2. Observed and simulated N_2O, WFPS and SOLT with a 95% total predictive uncertainty band in the (a) agriculture, (b) shelterbelt, and (c) grassland site. Error bars on the N_2O observations represent ±1.96 of the standard deviation, and those on WFPS and SOLT observations represent 10% measurement errors.

While MAE exceeded 20.0 gN/ha/day, low PBIAS (3.46%), near optimal NSE (0.89), RSR (0.33) and R^2 (0.89) suggest that the model represented the trend of observations. In the validation period, the model slightly underperformed. However, the qualitative rating remained the same. The relatively thin width of the 95% predictive uncertainty band (r-stat < 1.1) and the higher percentage of encapsulation of observations (p-stat > 0.63) further confirm the "very good" quality of model results.

As for the shelterbelt site, while the accuracy of SOLT and WFPS simulations are fairly comparable to that of the agricultural site, the quality of N_2O emission results has not been as promising. The model simulation frequently missed the observations (Fig. 2b), especially those observed in autumn months during both the calibration and validation periods. The goodness of fit statistics point to just a "satisfactory" quality of model results. PBIAS values are > -20%, low R^2 (<0.16), and relatively high MAE (>4.0 gN/ha/day) also confirm this. Furthermore, the lower performance of model simulation results is reflected in negative NSE (<-0.8) and high RSR (>1.34) values. Even in a relatively thick predictive uncertainty band (r-stat > 0.94), a lower percentage of the observations (p-stat < 0.5) fell within the band.

At the grassland site, which was subjected to very heavy grazing, the SOLT observations data were not available. The model captured the trend of WFPS observations (Fig. 2c) quite well, however it failed to replicate the observations during the autumn months of 2014, which led to just a "satisfactory" quality of model results in the calibration period. In the validation period, the WFPS results are of "very good" quality. While the model missed some of the high N_2O emission events, it represented the trend of observations fairly well, leading to "satisfactory" quality of model results during both calibration and validation periods. In the calibration period, acceptable values of PBIAS (−12.49%), MAE (0.49 gN/ha/yr), NSE (0.35), RSR (0.81) and R^2 (0.36) were obtained. The calculated p- and r-stat in the calibration period shows that the band could encapsulate only 36% of the observations. The goodness of fit statistics values for N_2O simulations worsened during the validation period.

3.2. Current and future spatiotemporal variability of N_2O emissions in the ARB

We re-optimized the N_2O related parameter values (Table S10) for soils with forest dominated land-use, as the regionalization of optimized parameter values obtained for the shelterbelt site significantly overestimated the emissions when compared to model-based estimates of Hashimoto (2012) at a sub-basin spatial scale (see discussion in §4.2). As for other land-use types (agriculture and grassland), we regionalized the site-based optimized parameter values. Furthermore, we validated the SWAT simulated SOLT and moisture (volumetric) with ERA-Interim reanalysis products (Dee et al., 2011), resampled at 0.05° over the entire ARB (Figures S2 and S3). While we are aware of the limitations of such reanalysis products (Jones et al., 2016), this validation would provide some insights into the accuracy of SWAT simulations. We calculated the R^2 between the SWAT simulation and the ERA-Interim reanalysis product, and found that the SOLT has been simulated with a "very good" accuracy while soil moisture (volumetric) simulation has been simulated with a wide range of accuracy ("unsatisfactory" to "good"). However, we did not attempt to re-calibrate the related SWAT parameters as we have already validated streamflow results at 35 gauging stations (Table S6). After regionalization, we also compared SWAT simulated emissions with model-based estimates of Hashimoto (2012), resampled at 0.05° (Figure S4). A wide range of accuracy ("very good" to "unsatisfactory") was observed. A higher accuracy was obtained at downstream regions (e.g. boreal plain) of the basin, where forest is the dominant land-use type (Fig. 1). At regions where agricultural activities are highest (e.g. Prairie and Lesser Slave), a lower accuracy was observed.

The N_2O emissions in the base-period (1990–2005) showed marked temporal and spatial variability in the ARB (Fig. 3, Table S11). With an annual emission of 2662 gN/ha/yr, agricultural land is the hot-spot of N_2O emissions in the ARB (Fig. 4, Table S13), driven mainly by the use of synthetic N fertilizer (Table 1), while forested areas contributed the lowest (141 gN/ha/yr). Evidently, the prairie (774 gN/ha/yr) and Lesser Slave (605 gN/ha/yr) regions contributed the highest levels to the basin scale N_2O budget, as these regions have the highest percentage of agricultural land (Fig. 1). The spring season has been the hot-moment for N_2O emissions in agricultural dominated regions (prairie and Lesser Slave), as this season alone contributes >50% to the annual N_2O budget, while summer season has been the hot-moment in forest dominated regions, such as in the boreal plain (Figure S6 and S7).

Compared to the base period, significant changes in N_2O emissions are projected in the future. Changes are land-use, region and season specific. In a drier-colder future climate, the annual emissions are projected to increase by +5% on a basin scale, with the highest increase (+21%) in the headwater region. This is mainly due to projected increases in emissions from forest land-use (+17%), as the emissions from the other land-use types would decrease (−3% to −28%). Consistent decreases in winter season emissions are expected (up to −92%) in all regions. While changes in spring and summer seasons are region specific, there are consistent increases in autumn season emissions (+2% to +20%). On the other hand, significant increases, irrespective of seasons and regions, are expected in a drier-warmer future climatic condition. The most significant increases are expected in the winter season, e.g. an increase by more than 15-fold in the headwater region. On the basin scale, the annual emissions would be up by +106%. While a similar trend has been observed for agriculture (+11%) and forest (+200%) land-use types, grassland (−4%) and pasture (−28%) showed the opposite. The share of winter, spring and autumn seasons to the annual emissions would increase. However, summer season would contribute less (Figure S8). The most significant decreases in emissions are expected in a wetter-colder future condition. As observed in a drier-colder example, the winter season emission would decrease significantly (up to −90%). Except in the headwater and foothill regions, decreases in spring (−14% to −25%), summer (−11% to −25%) and autumn (−1% to −12%) seasons emissions are expected in all other regions. Consequently, emissions from all the major land-use types would also decrease (−3% to −19%, Table S13). In a wetter-warmer future condition, while the emissions from agricultural land is expected to decrease by −12%, the emissions from all other major land-use types would increase, especially with +47% increases from forest land-use. Moreover, except in the Lesser Slave region in spring and summer seasons, the emissions in all seasons from other regions would increase, resulting in an increase of +13% in annual emissions. We found this increment (+13%) significantly lower than that observed in a drier-warmer scenario (+106%). Similarly, the increase (+13%) is significantly higher than that observed in a wetter-colder case (−19%). This shows that a wetter future might not always accelerate emissions, however, a warmer future definitely would do.

3.3. Effect of different management scenarios on N_2O emission of the ARB

In the agricultural area, split fertilizer applications (Sc-1, Table 1) would slightly increase (+0.02% from agricultural land-use, 3% on basin scale) emissions (Fig. 5). As expected, a lower dose of fertilizer

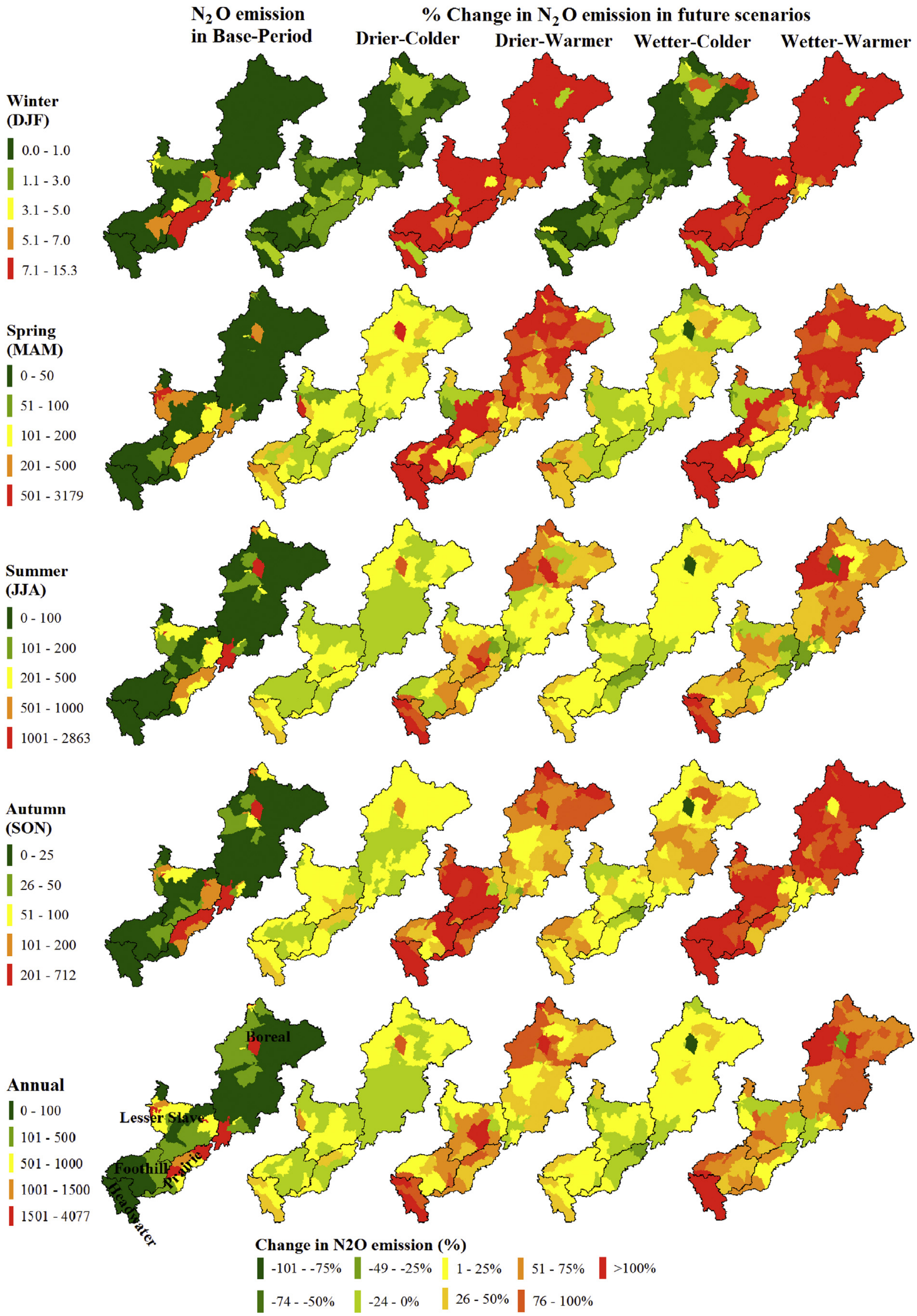

Fig. 3. Annual and seasonal N_2O emissions (g/ha) in the base case and percentage changes in future cases in the Athabasca River Basin.

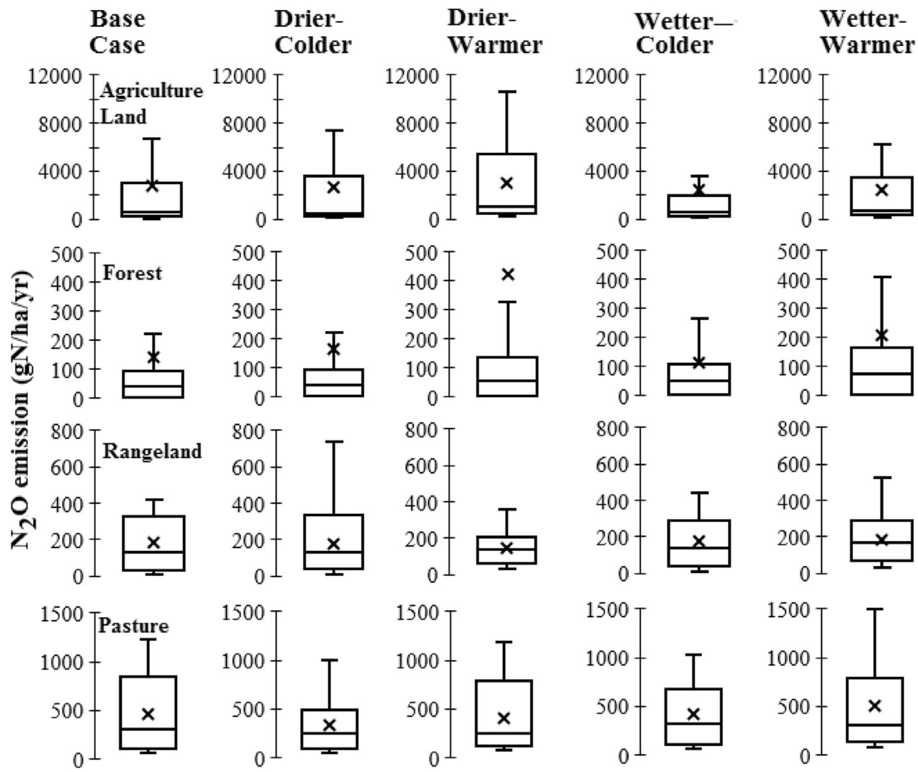

Fig. 4. Box-plots of annual N_2O emissions in the base and future cases in different land-use types in the Athabasca River Basin.

application (Sc-2) would decrease emissions substantially (−24% from agricultural land-use, −20% on basin scale). A combination of a lower dose of fertilizer and split applications (Sc-3) would have negligible effect on the emission as compared to the previous scenario (Sc-2). We observed significant changes in emissions while adopting different crop residue management practices. When assigning residue harvest index (HI_OVR) with the stover fraction removed (FRAC_HARVK) a value of 1% (Sc-4a), leaving 99% crop residue in the field, the increase in emissions would be as high as +198%. On the other hand, managing 75% and 99% of crop residue (Sc-4b&4c) would decrease emissions by −37% and −65% respectively, which would translate to −18% and −34%, on the basin scale. As for pasture, adopting the lowest recommended dose of fertilizer (Sc-5) would substantially decrease (−61%) emissions, which contributes only a −1% reduction on a basin scale. Similarly, limiting grazing intensity (Sc-6) on the grassland land-use to "light grazing" would decrease emissions quite significantly (−39%), but would translate to only-1% on the basin scale.

4. Discussion

4.1. Challenges in N_2O emissions modelling in cold climate river basins

In general, the accuracy of these model results is comparable to other similar studies (Iqbal et al., 2018; Smith et al., 2002; Wagena et al., 2017; Yang et al., 2017). Table S14 shows comparison of goodness-of-fit statistics obtained in this study with that reported in Wagena et al. (2017); Yang et al. (2017), all of which have used the SWAT model, thereby allowing a direct comparison. For most of the cases, the model has simulated SOLT and WFPS with a higher accuracy than N_2O. A higher accuracy of SOLT simulation was expected due to its direct dependence on air temperature, which can be measured at a high accuracy and the spatial variability of air temperature is rather low (Whitfield et al., 2002). As for WFPS, results showed that a relatively higher quality of simulation can be achieved after careful parameterization of snow-related processes in cold climate regions, especially considering the errors in precipitation measurements (Metcalfe et al., 1997) and the spatial variability of precipitation (Whitfield et al., 2002). The importance of robust precipitation data for better WFPS simulations was also reflected at the grassland site, in which the model failed to capture observed WFPS observations, especially during the September to November period of 2014 (Fig. 2c). This mismatch can be attributed to the precipitation data as it is clear that, during the period, no significant precipitation pulses (precipitation < 5 mm/day) were recorded and the model adequately reflected this, but the WFPS observations showed increments from 0.2 to 0.4.

Furthermore, with similar accuracies of SOLT and WFPS simulations at all three sites, the accuracy of N_2O simulations varied profoundly. For the cropped site, as the timing of the fertilizer applications was unknown, we treated this as a calibration parameter, keeping the total fertilizer application as reported (Amadi et al., 2016) (refer Table S9). This illustrates that, if precise information on the amount and timing of fertilizer applications is obtained, and if the qualities of SOLT and WFPS simulations are good, the model can re-produce the N_2O with a high accuracy. In fact, a lower quality of N_2O results at the shelterbelt site (Fig. 2b) and grassland site (Fig. 2c) can also be attributed to this. Given that there was no evidence of the use of any synthetic N fertilizers in the shelterbelt site (Amadi et al., 2016), the magnitude of observed N_2O emissions (as high as 25 gN/ha/day) appears to be quite high when compared to the emissions from a heavily grazed grassland site (Fig. 2c, N_2O level has never crossed 10 gN/ha/day). Note that the grassland site receives cattle dung and urine deposited by grazing cattle. As the shelterbelt site is adjacent to the cropped site, the fertilizer applied to the agriculture site might have been leached, thereby maintaining a high concentration of substrates in the soil, which in turn

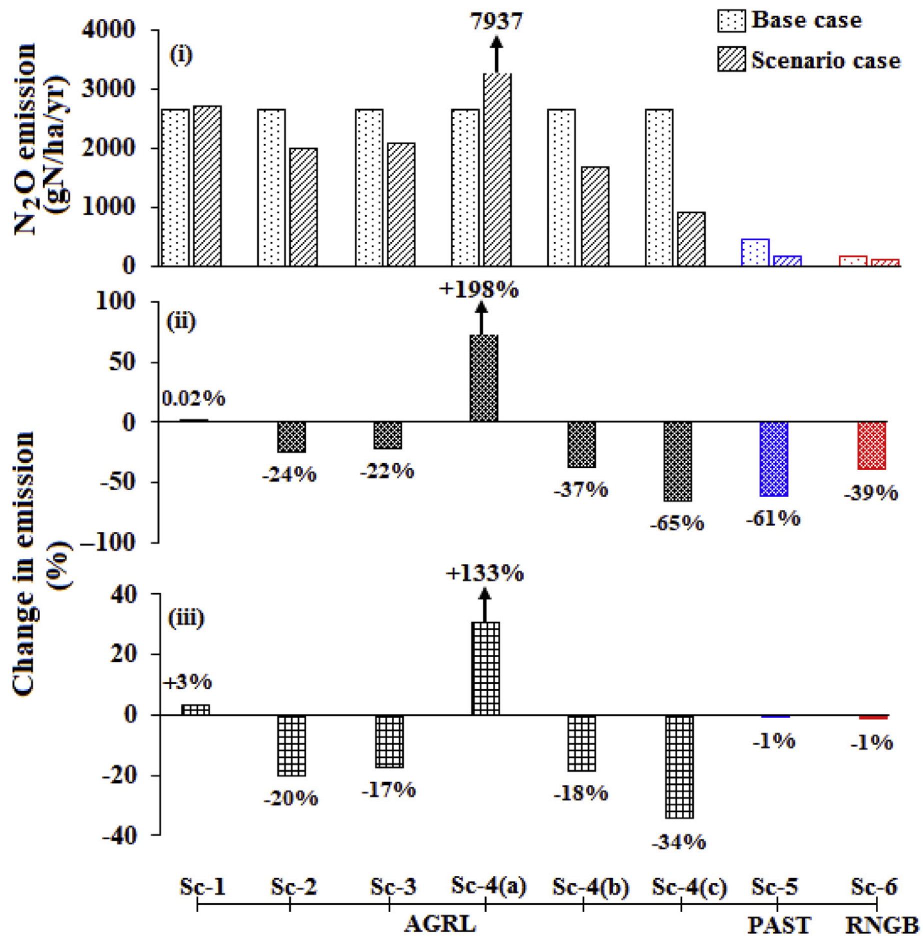

Fig. 5. (i) Annual emissions (g/ha/yr) from specific land-use types in base and different scenario cases; percentage changes in emissions from (ii) specific land-use types, and (iii) the Athabasca River Basin. AGRL: agriculture land, PAST: pasture and RNGB: grassland. Refer to Table 1 for details on each scenario (Sc-1 to Sc-6).

resulted in the high emission peaks. Devoid of reliable and correct information, we could not impose any synthetic N fertilizer amount to the model. On the other hand, these high N_2O emissions could be due to so called "microscale N_2O emissions" in plant residue-induced hotspots as a result of micro-environmental conditions, which could be different than those found in bulk soil (Kravchenko et al., 2017). These hot-spots are primarily due to high WFPS levels within the plant residue (Kravchenko et al., 2017). It is obvious that we did not incorporate such microscale processes in our current implementation. As can be seen in Fig. 2b, during the autumn period of 2013, four consecutive measurements showed rather high emissions despite lower values of WFPS (~0.2, and the model has accurately simulated them). At such low WFPS, it is shown that N_2O emissions from denitrification ceases (Weier et al., 1993), and a lower WFPS reduction factor for nitrification related emissions should obviously make the simulated emission rather low. Therefore, the evidence of such high observations also supports the likely presence of plant residue-induced hotspots. At the grassland site, mismatching of higher N_2O emissions, especially during the validation period (Fig. 2c) might be related to measurements from a patch with highly concentrated cattle dung and urine. Especially the urine, which contains a high percentage of NH_4 that ultimately undergoes ammonia oxidation and nitrification reactions to produce NO_3, which is highly susceptible to denitrification (Thomas et al., 2017). In SWAT, faecal material deposition from grazing animals is assumed to be distributed uniformly, and such patches are not considered in the model.

As shown by various studies, the N_2O emissions in such cold climate regions during freeze-thaw cycles constitute the emission hot-moments (Flechard et al., 2005; McClain et al., 2003; Pelster et al., 2013). While some sporadic data at the cropped and shelterbelt sites were available when the soil temperatures are around freezing (Fig. 2a and b), we lacked data in such periods at the grassland site (Fig. 2c). Therefore, there was a lower confidence in simulated N_2O pulses during the early freeze-thaw cycle from the site. In general, a lack of continuous measurements constrained the model validation at all sites. We are aware that the difficulties in collecting such datasets will continue unless an automated system is made available (Smith and Dobbie, 2001). Furthermore, a high diurnal variability of the emissions exists as shown by the large error bars on the observations (Fig. 2a–c), which indicates that the N_2O emission process is rather dynamic. Also, that the use of a daily time scale in the SWAT model might be inappropriate as the model would fail to capture the emissions that might have taken place in a sub-daily time scale, such as in a brief and intense precipitation event (Iqbal et al., 2018). Moreover, errors and uncertainties associated with gas chamber measurements are well reported (Smith and Dobbie, 2001; Venterea et al., 2009).

4.2. Implications of upscaling site-based parameters to watershed scale

The benefits of model parameter regionalization are well illustrated and widely practiced (Gitau and Chaubey, 2010; Merz and

Blöschl, 2004). As already shown, due to the lack of N_2O measurements at the ARB, we have regionalized N_2O related parameters (Table S4), optimized from site-based measurements at the watershed scale. However, our results suggest that caution should be used in doing so. For instance, the best-fit value of parameters; K9 (represented as K2 in Eqn. (4)) and K7 (represented as K_{max} in Eqn. (5)) for the shelterbelt site was found to be higher than those optimized for both the agriculture and grassland sites. In the shelterbelt site, soil NO_3 concentration was rather low (Amadi et al., 2016) as there was no synthetic N fertilizer input. Furthermore, it has been shown that the N_2O emissions from denitrification are generally limited by NO_3 concentrations (Luo et al., 1998). However, observations showed relatively high N_2O emissions. The SWAT-CUP (Abbaspour et al., 2004) based auto-optimization algorithm that we applied in this study would seek for a parameter combination that would result in the highest possible value of the chosen objective function. Hence, we believe that the optimized parameter values for the shelterbelt site are not reliable and required re-optimization. Histograms (Figure S5) of re-optimized parameter values (R7 and R9) also confirmed this.

4.3. Climate change and N_2O emission

Withstanding the impacts of changes in precipitation and temperature on environmental variables (e.g. SOLT and WFPS), soil erosion, nutrients (e.g. NH_4, NO_3, etc.), and crop dynamics, the effects on emissions are expected to be non-linear and non-stationary. In the ARB, the warmer conditions are more sensitive than the wetter conditions for emissions and the combined effect of a wetter and warmer future was offsetting rather than synergetic.

In a warmer future condition, early snow freshet led to increased winter season emissions and decreased spring season emissions in some regions of the basin (e.g. Lesser Slave, Table S11), mainly due to fluctuations in the WFPS. Furthermore, consistent increases in summer and autumn season emissions across all regions, in a warmer condition, was due to greater residue decomposition, thereby increasing substrate concentrations. Moreover, warmer conditions would lead to higher temperature reduction factors (Eqns. S6 and S13). Moreover, elevated temperatures are shown to increase plant biomass in the ARB, mainly due to lower temperature stress (Shrestha et al., 2017; Shrestha and Wang, 2018), which also helps to increase the plant residue in soil. In a wetter future condition, nitrogen losses from soils would be exacerbated as the nitrogen concentration in surface runoff, along with lateral and groundwater flows, would increase (Table S12). Furthermore, there would be increases in sediment associated nutrient loss. Due to limited substrate concentrations, N_2O emissions from both nitrification and denitrification would decrease. This further highlights the need for a modelling tool that can consider interactions among soil, water, vegetation, and nutrients, including the lateral transport of water and nutrients. Moreover, the optimal value for the WFPS reduction factor (Eqn. (S34)) for nitrification induced N_2O emission would be approximately 0.6 (Parton et al., 2001). This implies that a wetter condition would further increase WFPS, which would in turn decrease nitrification related emissions.

4.4. Plausible N_2O emission abatement scenarios

Slight increases in the emissions in split fertilizer applications when compared to a single application of an economically optimal (AGRI-FACTS, 2013) dose could be due to higher N loss in later applications when encountered with an intense precipitation event. Furthermore, it has been shown that split N-applications would increase grain yield and protein content (Fischer et al., 1993), and decomposition of a higher amount of crop residue would lead to the slightest of the increases. The significant decreases in emissions when adopting the lower limit of the recommended dose of fertilizer in Alberta (AGRI-FACTS, 2004) is notable, as studies have shown that reducing synthetic N-input induces little compromise in crop yield (Hoben et al., 2011; McSwiney and Robertson, 2005). This also highlights the opportunity for reducing emissions from normal fertilizer applications and management (Gerber et al., 2016). Increasing efficiency in crop residue harvest and management with stover removal, are shown to result in reduced soil moisture, winter soil temperature and soil carbon levels, and in increased summer soil temperature and crop yield (Kenney et al., 2015), which should result in significant decreases in emissions. In literature, even though contrasting results have been seen as to the extent that crop residue would change the emission levels, we observed stimulatory effects of crop residue on N_2O emissions, akin to manure application in the study of Zhou et al. (2017). Our model based estimates of such significant decreases in the emission (−18% for stover removal of 75% and −34% for stover removal of 99%) are indeed higher than most of the reported values such as −7% (on average) decrease for high residue removal (up to 75%) by Jin et al. (2014), −20% decrease (annual emission of 3.5 to 2.8 kgN_2O-N/ha) for high residue removal (up to 75%) by Jin et al. (2017), −4.8% decrease (annual emission of 1.25 to 1.19 kg N_2O-N/ha) by Baker et al. (2014), among other. Some studies, e.g. (Baker et al., 2014; Campbell et al., 2014; Chen et al., 2013; Jin et al., 2017; Pelster et al., 2013; Shan and Yan, 2013; Velthof et al., 2002), however, reported the changes to be 'statistically insignificant'. Hence, this issue indeed needs further investigation.

Acknowledgement

The authors would like to thank the Alberta Economic Development and Trade for the Campus Alberta Innovates Program Research Chair (No. RCP-12-001-BCAIP). We would also like to thank Mr. J. Sellers for proofreading; M. Wagena and co-authors, and Q. Yang and co-authors for sharing their version of SWAT codes. The authors would also like to thank four anonymous reviewers for providing insightful comments which helped immensely to improve the quality of this study.

Appendix A. Supplementary data

Supplementary data related to this article can be found at https://doi.org/10.1016/j.envpol.2018.04.068.

References

AAF, 2017. Wheat Nutrition and Fertilizer Requirements: Nitrogen. Alberta Agriculture and Forestry (AAF), Edmonton, Alberta, Canada.
Abalos, D., Cardenas, L.M., Wu, L., 2016. Climate change and N2O emissions from South West England grasslands: a modelling approach. Atmos. Environ. 132, 249–257.
Abbaspour, K.C., Johnson, C.A., van Genuchten, M.T., 2004. Estimating uncertain flow and transport parameters using a sequential uncertainty fitting procedure. Vadose Zone J. 3, 1340–1352.
Abbaspour, K.C., Rouholahnejad, E., Vaghefi, S., Srinivasan, R., Yang, H., Kløve, B., 2015. A continental-scale hydrology and water quality model for Europe: calibration and uncertainty of a high-resolution large-scale SWAT model. J. Hydrol. 524, 733–752.
AGRI-FACTS, 1998. Grazing tame pastures effectively. In: AGRI-FACTS. Alberta Agriculture and Forestry, Edmonton, Canada.
AGRI-FACTS, 2004. Alberta fertilizer guide. In: AGRI-FACTS. Alberta Agriculture and Forestry, Edmonton, Canada.
AGRI-FACTS, 2013. Dryland agronomic management of soft white spring wheat and Canada prairie spring wheat in Alberta. In: AGRI-FACTS. Alberta Agriculture and Forestry, Edmonton, Canada.
AGRI-FACTS, 2005a. Fertilizing grass for hay and pasture. In: AGRI-FACTS. Alberta Agriculture and Forestry, Edmonton, Canada.
AGRI-FACTS, 2005b. Perennial forage establishment in alberta. In: AGRI-FACTS. Alberta Agriculture and Forestry, Edmonton, Canada.

Amadi, C.C., Van Rees, K.C.J., Farrell, R.E., 2016. Soil–atmosphere exchange of carbon dioxide, methane and nitrous oxide in shelterbelts compared with adjacent cropped fields. Agric. Ecosyst. Environ. 223, 123–134.
Arnold, J.G., Moriasi, D.N., Gassman, P.W., Abbaspour, K.C., White, M.J., Srinivasan, R., Santhi, C., Harmel, R.D., van Griensven, A., Van Liew, M.W., Kannan, N., Jha, M.K., 2012. SWAT: model use, calibration, and validation. Am. Soc. Agric. Biol. Eng. 55, 18.
Arnold, J.G., Srinivasan, R., Muttiah, R.S., Williams, J.R., 1998. Large area hydrologic modeling and assessment part I: model development. J. Am. Water Resour. Assoc. 34, 73–89.
Arnold, J.G., Kiniry, J.R., Srinivasan, R., Williams, J.R., Haney, E.B., Neitsch, S.L., 2011. Soil and Water Assessment Tool Input/Output File Documentation, Version 2009. Agrilife Blackland Research Center, Temple, Texas, p. 76502.
AWC, 2013. State of the Watershed Report: Phase 3-Water Quantity and Basic Water Quality in the Athabasca Watershed. Athabasca Watershed Council.
AWC, 2014. Athabasca State of the Watershed Assessment Phase 4: Organic Compounds in Surface Water and Sediments, and Trace Metals in Sediments. Athabasca Watershed Council.
Baker, J.M., Fassbinder, J., Lamb, J.A., 2014. The impact of corn stover removal on N2O emission and soil respiration: an investigation with automated chambers. BioEnergy Res. 7, 503–508.
Best, M.J., Pryor, M., Clark, D.B., Rooney, G.G., Essery, R.L.H., Ménard, C.B., Edwards, J.M., Hendry, M.A., Porson, A., Gedney, N., Mercado, L.M., Sitch, S., Blyth, E., Boucher, O., Cox, P.M., Grimmond, C.S.B., Harding, R.J., 2011. The joint UK land environment simulator (JULES), model description – Part 1: energy and water fluxes. Geosci. Model Dev. (GMD) 4, 677–699.
Black, P.E., 1997. Watershed functions. J. Am. Water Resour. Assoc. 33, 1–11.
Butterbach-Bahl, K., Baggs, E.M., Dannenmann, M., Kiese, R., Zechmeister-Boltenstern, S., 2013. Nitrous oxide emissions from soils: how well do we understand the processes and their controls? Phil. Trans. Roy. Soc. Biol. Sci. 368.
Campbell, E.E., Johnson, J.M.F., Jin, V.L., Lehman, R.M., Osborne, S.L., Varvel, G.E., Paustian, K., 2014. Assessing the soil carbon, biomass production, and nitrous oxide emission impact of corn stover management for bioenergy feedstock production using DAYCENT. BioEnergy Res. 7, 491–502.
CFSR, 2016. Climate Forecast System Reanalysis. http://globalweather.tamu.edu/G.W.D.f.S.T.A.M.U.I.
Chen, H., Li, X., Hu, F., Shi, W., 2013. Soil nitrous oxide emissions following crop residue addition: a meta-analysis. Global Change Biol. 19, 2956–2964.
Clark, D.B., Mercado, L.M., Sitch, S., Jones, C.D., Gedney, N., Best, M.J., Pryor, M., Rooney, G.G., Essery, R.L.H., Blyth, E., Boucher, O., Harding, R.J., Huntingford, C., Cox, P.M., 2011. The Joint UK Land Environment Simulator (JULES), model description – Part 2: carbon fluxes and vegetation dynamics. Geosci. Model Dev. (GMD) 4, 701–722.
Coleman, K., Jenkinson, D.S., 1996. RothC-26.3-A Model for the turnover of carbon in soil. In: Powlson, D.S., Smith, P., Smith, J.U. (Eds.), Evaluation of Soil Organic Matter Models. Springer, Berlin.
Dee, D.P., Uppala, S.M., Simmons, A.J., Berrisford, P., Poli, P., Kobayashi, S., Andrae, U., Balmaseda, M.A., Balsamo, G., Bauer, P., Bechtold, P., Beljaars, A.C.M., van de Berg, L., Bidlot, J., Bormann, N., Delsol, C., Dragani, R., Fuentes, M., Geer, A.J., Haimberger, L., Healy, S.B., Hersbach, H., Hólm, E.V., Isaksen, L., Kållberg, P., Köhler, M., Matricardi, M., McNally, A.P., Monge-Sanz, B.M., Morcrette, J.J., Park, B.K., Peubey, C., de Rosnay, P., Tavolato, C., Thépaut, J.N., Vitart, F., 2011. The ERA-Interim reanalysis: configuration and performance of the data assimilation system. Q. J. R. Meteorol. Soc. 137, 553–597.
Del Grosso, S.J., Parton, W.J., 2012. Climate change increases soil nitrous oxide emissions. New Phytol. 196, 327–328.
Del Grosso, S.J., Parton, W.J., Mosier, A.R., Hartman, M.D., Keough, C.A., Peterson, G.A., Ojima, D.S., Schimel, D.S., 2001. Simulated effects of land use, soil texture, and precipitation on N gas emissions using DAYCENT. In: Follett, R.F., Hatfield, J.L. (Eds.), Nitrogen in the Environment: Sources, Problems, and Management. Elsevier Science Publishers, The Netherlands, pp. 413–431.
Eric, A.D.a.D.K., 2014. Inventories and scenarios of nitrous oxide emissions. Environ. Res. Lett. 9, 105012.
Eum, H.-I., Dibike, Y., Prowse, T., 2017. Climate-induced alteration of hydrologic indicators in the Athabasca River basin, Alberta, Canada. J. Hydrol. 544, 327–342.
Fischer, R.A., Howe, G.N., Ibrahim, Z., 1993. Irrigated spring wheat and timing and amount of nitrogen fertilizer. I. Grain yield and protein content. Field Crop. Res. 33, 37–56.
Flechard, C.R., Neftel, A., Jocher, M., Ammann, C., Fuhrer, J., 2005. Bi-directional soil/atmosphere N2O exchange over two mown grassland systems with contrasting management practices. Global Change Biol. 11, 2114–2127.
Gao, X., Thomas, B.W., Beck, R., Thompson, D.J., Zhao, M., Willms, W.D., Hao, X., 2018. Long-term grazing alters soil trace gas fluxes from grasslands in the foothills of the Rocky Mountains, Canada. Land Degrad. Dev. 29, 292–302.
Gerber, J.S., Carlson, K.M., Makowski, D., Mueller, N.D., Garcia de Cortazar-Atauri, I., Havlík, P., Herrero, M., Launay, M., O'Connell, C.S., Smith, P., West, P.C., 2016. Spatially explicit estimates of N2O emissions from croplands suggest climate mitigation opportunities from improved fertilizer management. Global Change Biol. 22, 3383–3394.
Giorgi, F., Bi, X., 2005. Regional changes in surface climate interannual variability for the 21st century from ensembles of global model simulations. Geophys. Res. Lett. 32.
Gitau, M.W., Chaubey, I., 2010. Regionalization of SWAT model parameters for use in ungauged watersheds. Water 2, 849–871.
GoC, 2016. Environment and Natural Resources; Weather, Climate and Hazard. http://climate.weather.gc.ca/. G.o.C.
Groffman, P.M., Butterbach-Bahl, K., Fulweiler, R.W., Gold, A.J., Morse, J.L., Stander, E.K., Tague, C., Tonitto, C., Vidon, P., 2009. Challenges to incorporating spatially and temporally explicit phenomena (hotspots and hot moments) in denitrification models. Biogeochemistry 93, 49–77.
Hashimoto, S., 2012. A new estimation of global soil greenhouse gas fluxes using a simple data-oriented model. PLoS One 7 e41962.
Hawkins, E., Sutton, R., 2009. The potential to narrow uncertainty in regional climate predictions. Bull. Am. Meteorol. Soc. 90, 1095–1107.
Helbig, M., Chasmer, L.E., Kljun, N., Quinton, W.L., Treat, C.C., Sonnentag, O., 2017. The positive net radiative greenhouse gas forcing of increasing methane emissions from a thawing boreal forest-wetland landscape. Global Change Biol. 23, 2413–2427.
Hoben, J.P., Gehl, R.J., Millar, N., Grace, P.R., Robertson, G.P., 2011. Nonlinear nitrous oxide (N2O) response to nitrogen fertilizer in on-farm corn crops of the US Midwest. Global Change Biol. 17, 1140–1152.
IPCC, 2006. IPCC Guidelines for National Greenhouse Gas Inventories. Institute for Global Environmental Strategies (IGES), Hayama, Japan, Hayama, Japan, p. 2006.
IPCC, 2007. Climate Change 2007: Impacts, Adaptation and Vulnerability. Contribution of Working Group II to the Fourth Assessment Report of the Intergovernmental Panel on Climate Change. Cambridge University Press, Cambridge, U.K.
IPCC, 2014. Climate Change 2014: Synthesis Report. Contribution of Working Groups I, II and III to the Fifth Assessment Report of the Intergovernmental Panel on Climate Change. In: Core Writing Team, R.K.P.a.L.A.M.e., p. 151. IPCC, IPCC.
Iqbal, J., Necpalova, M., Archontoulis, S.V., Anex, R.P., Bourguignon, M., Herzmann, D., Mitchell, D.C., Sawyer, J.E., Zhu, Q., Castellano, M.J., 2018. Extreme weather-year sequences have nonadditive effects on environmental nitrogen losses. Global Change Biol. 24, e303–e317.
Jarvis, A., Reuter, H.I., Nelson, A., Guevara, E., 2008. Hole-filled SRTM for the Globe Version 4, Available from the CGIAR-csi SRTM 90m Database. CGIAR. http://srtm.csi.cgiar.org.
Jin, V.L., Baker, J.M., Johnson, J.M.F., Karlen, D.L., Lehman, R.M., Osborne, S.L., Sauer, T.J., Stott, D.E., Varvel, G.E., Venterea, R.T., Schmer, M.R., Wienhold, B.J., 2014. Soil Greenhouse Gas Emissions in Response to Corn Stover Removal and Tillage Management Across the US Corn Belt. BioEnergy Res. 7, 517–527.
Jin, V.L., Schmer, M.R., Stewart, C.E., Sindelar, A.J., Varvel, G.E., Wienhold, B.J., 2017. Long-term no-till and stover retention each decrease the global warming potential of irrigated continuous corn. Global Change Biol. 23, 2848–2862.
Jones, R.W., Renfrew, I.A., Orr, A., Webber, B.G.M., Holland, D.M., Lazzara, M.A., 2016. Evaluation of four global reanalysis products using in situ observations in the Amundsen Sea Embayment, Antarctica. J. Geophys. Res.: Atmosphere 121, 6240–6257.
Kannan, N., White, S.M., Worrall, F., Whelan, M.J., 2006. Pesticide Modelling for a Small Catchment Using SWAT-2000. J. Environ. Sci. Health Part B 41, 1049–1070.
Kanter, D.R., Zhang, X., Mauzerall, D.L., Malyshev, S., Shevliakova, E., 2016. The importance of climate change and nitrogen use efficiency for future nitrous oxide emissions from agriculture. Environ. Res. Lett. 11, 094003.
Kenney, I., Blanco-Canqui, H., Presley, D.R., Rice, C.W., Janssen, K., Olson, B., 2015. Soil and crop response to stover removal from rainfed and irrigated corn. GCB Bioenergy 7, 219–230.
Khanna, M., Paulson, N., 2016. To Harvest Stover or Not: Is it Worth it? Farmdoc Daily 6, 32.
Kravchenko, A.N., Toosi, E.R., Guber, A.K., Ostrom, N.E., Yu, J., Azeem, K., Rivers, M.L., Robertson, G.P., 2017. Hotspots of soil N2O emission enhanced through water absorption by plant residue. Nat. Geosci. 10, 496.
Kurylyk, B.L., MacQuarrie, K.T.B., McKenzie, J.M., 2014. Climate change impacts on groundwater and soil temperatures in cold and temperate regions: Implications, mathematical theory, and emerging simulation tools. Earth Sci. Rev. 138, 313–334.
Leta, O.T., Shrestha, N.K., de Fraine, B., van Griensven, A., Bauwens, W., 2014. Integrated Water Quality Modelling of the River Zenne (Belgium) Using OpenMI. In: Gourbesville, P., Cunge, J., Caignaert, G. (Eds.), Advances in Hydroinformatics: SIMHYDRO 2012 – New Frontiers of Simulation. Springer Singapore, Singapore, pp. 259–274.
Li, C., Frolking, S., Frolking, T.A., 1992. A model of nitrous oxide evolution from soil driven by rainfall events: 1. Model structure and sensitivity. J. Geophys. Res.: Atmosphere 97, 9759–9776.
Liao, T., Wang, R., Zheng, X., Sun, Y., Butterbach-Bahl, K., Chen, N., 2013. Automated online measurement of N2, N2O, NO, CO2, and CH4 emissions based on a gas-flow-soil-core technique. Chemosphere 93, 2848–2853.
Ligaray, M., Kim, M., Baek, S., Ra, J.-S., Chun, A.J., Park, Y., Boithias, L., Ribolzi, O., Chon, K., Cho, H.K., 2017. Modeling the Fate and Transport of Malathion in the Pagsanjan-Lumban Basin, Philippines. Water 9.
Luo, J., Tillman, R.W., White, R.E., Ball, P.R., 1998. Variation in denitrification activity with soil depth under pasture. Soil Biol. Biochem. 30, 897–903.
Lutz, A.F., ter Maat, H.W., Biemans, H., Shrestha, A.B., Wester, P., Immerzeel, W.W., 2016. Selecting representative climate models for climate change impact studies: an advanced envelope-based selection approach. Int. J. Climatol. 36, 3988–4005.
McClain, M.E., Boyer, E.W., Dent, C.L., Gergel, S.E., Grimm, N.B., Groffman, P.M., Hart, S.C., Harvey, J.W., Johnston, C.A., Mayorga, E., McDowell, W.H., Pinay, G.,

2003. Biogeochemical Hot Spots and Hot Moments at the Interface of Terrestrial and Aquatic Ecosystems. Ecosystems 6, 301–312.
McSwiney, C.P., Robertson, G.P., 2005. Nonlinear response of N2O flux to incremental fertilizer addition in a continuous maize (Zea mays L.) cropping system. Global Change Biol. 11, 1712–1719.
Meng, Y., Zhou, L., He, S., Lu, C., Wu, G., Ye, W., Ji, P., 2018. A heavy metal module coupled with the SWAT model and its preliminary application in a mine-impacted watershed in China. Sci. Total Environ. 613–614, 1207–1219.
Merz, R., Blöschl, G., 2004. Regionalisation of catchment model parameters. J. Hydrol. 287, 95–123.
Metcalfe, J.R., Routledge, B., Devine, K., 1997. Rainfall Measurement in Canada: Changing Observational Methodsand Archive Adjustment Procedures. J. Clim. 10, 92–101.
Moriasi, D.N., Arnold, J.G., Van Liew, M.W., Binger, R.L., Harmel, R.D., Veith, T., 2007. Model evaluation guidelines for systematic quantification of accuracy in watershed simulations. Trans. ASABE 50, 885–900.
Moriasi, D.N., Gitau, M.W., Pai, N., Daggupati, P., 2015. Hydrologic and Water Quality Models: Performance Measures and Evaluation Criteria, vol. 58.
Murdock, T.Q., Cannon, A.J., Sobie, S.R., 2013. Statistical Downscaling of Future Climate Projections. Pacific Climate Impacts Consortium (PCIC), Victoria, British Columbia, Canada.
Nash, J.E., Sutcliffe, J.V., 1970. River flow forecasting through conceptual models part I — A discussion of principles. J. Hydrol. 10, 282–290.
Neitsch, S.L., Arnold, J.G., Kiniry, J.R., Williams, J.R., 2011. Soil & Water Assessment Tool Theoretical Documentation, Version 2009. Grassland,Soil and Water Research Laboratory-agricultural Research Service. Blackland Research Center-Texas AgriLife Research.
Olefeldt, D., Roulet, N.T., 2014. Permafrost conditions in peatlands regulate magnitude, timing, and chemical composition of catchment dissolved organic carbon export. Global Change Biol. 20, 3122–3136.
Parton, W.J., 1996. The CENTURY model. In: Powlson, D.S., Smith, P., Smith, J.U. (Eds.), Evaluation of Soil Organic Matter Models. Springer, Berlin.
Parton, W.J., Holland, E.A., Del Grosso, S.J., Hartman, M.D., Martin, R.E., Mosier, A.R., Ojima, D.S., Schimel, D.S., 2001. Generalized model for NO x and N2O emissions from soils. J. Geophys. Res.: Atmosphere 106, 17403–17419.
Parton, W.J., Mosier, A.R., Ojima, D.S., Valentine, D.W., Schimel, D.S., Weier, K., Kulmala, A.E., 1996. Generalized model for N2 and N2O production from nitrification and denitrification. Global Biogeochem. Cycles 10, 401–412.
Pelster, D.E., Chantigny, M.H., Rochette, P., Angers, D.A., Laganière, J., Zebarth, B., Goyer, C., 2013. Crop residue incorporation alters soil nitrous oxide emissions during freeze–thaw cycles. Can. J. Soil Sci. 93, 415–425.
Raich, J.W., Tufekciogul, A., 2000. Vegetation and soil respiration: Correlations and controls. Biogeochemistry 48, 71–90.
Rofner, C., Peter, H., Catalán, N., Drewes, F., Sommaruga, R., Pérez, M.T., 2017. Climate-related changes of soil characteristics affect bacterial community composition and function of high altitude and latitude lakes. Global Change Biol. 23, 2331–2344.
Scarlat, N., Martinov, M., Dallemand, J.-F., 2010. Assessment of the availability of agricultural crop residues in the European Union: Potential and limitations for bioenergy use. Waste Manag. 30, 1889–1897.
Schmid, M., Neftel, A., Riedo, M., Fuhrer, J., 2001. Process-based modelling of nitrous oxide emissions from different nitrogen sources in mown grassland. Nutrient Cycl. Agroecosyst. 60, 177–187.
Schuur, E.A.G., McGuire, A.D., Schädel, C., Grosse, G., Harden, J.W., Hayes, D.J., Hugelius, G., Koven, C.D., Kuhry, P., Lawrence, D.M., Natali, S.M., Olefeldt, D., Romanovsky, V.E., Schaefer, K., Turetsky, M.R., Treat, C.C., Vonk, J.E., 2015. Climate change and the permafrost carbon feedback. Nature 520, 171.
Shan, J., Yan, X., 2013. Effects of crop residue returning on nitrous oxide emissions in agricultural soils. Atmos. Environ. 71, 170–175.
Shrestha, N.K., Du, X., Wang, J., 2017. Assessing climate change impacts on fresh water resources of the Athabasca River Basin, Canada. Sci. Total Environ. 601–602, 425–440.
Shrestha, N.K., Leta, O.T., De Fraine, B., Garcia-Armisen, T., Ouattara, N.K., Servais, P., van Griensven, A., Bauwens, W., 2014. Modelling Escherichia coli dynamics in the river Zenne (Belgium) using an OpenMI based integrated model. J. Hydroinf. 16, 354–374.
Shrestha, N.K., Leta, O.T., De Fraine, B., van Griensven, A., Bauwens, W., 2013. OpenMI-based integrated sediment transport modelling of the river Zenne, Belgium. Environ. Model. Software 47, 193–206.
Shrestha, N.K., Wang, J., 2017. Hydrological Modeling of Athabasca River Basin, Canada using Soil and Water Assessment Tool (SWAT). In: GeoConvention, May 18-19, 2017, Calgary, Alberta, Canada.
Shrestha, N.K., Wang, J., 2018. Predicting sediment yield and transport dynamics of a cold climate region watershed in changing climate. Sci. Total Environ. 625, 1030–1045.
Shrestha, N.K., Wang, J., Accepted. Water Quality Management of a Cold Climate Region Watershed in Changing Climate. Journal of Environmental Informatics.
SLC, 2010. Soil Landscapes of Canada Version 3.2. http://sis.agr.gc.ca/cansis/nsdb/slc/v3.2/index.html. A.a.A.-f.C.
Smith, K.A., Dobbie, K.E., 2001. The impact of sampling frequency and sampling times on chamber-based measurements of N2O emissions from fertilized soils. Global Change Biol. 7, 933–945.
Smith, W.N., Desjardins, R.L., Grant, B., Li, C., Lemke, R., Rochette, P., Corre, M.D., Pennock, D., 2002. Testing the DNDC model using N2O emissions at two experimental sites in Canada. Can. J. Soil Sci. 82, 365–374.
Tesi, T., Muschitiello, F., Smittenberg, R.H., Jakobsson, M., Vonk, J.E., Hill, P., Andersson, A., Kirchner, N., Noormets, R., Dudarev, O., Semiletov, I., Gustafsson, Ö., 2016. Massive remobilization of permafrost carbon during post-glacial warming. Nat. Commun. 7, 13653.
Thomas, B.W., Gao, X., Stoeckli, J.L., Beck, R., Liu, K., Koenig, K.M., Beres, B.L., Hao, X., 2017. Nitrapyrin reduced nitrous oxide emissions from beef cattle urine patches on a semiarid tame pasture. Soil Sci. Soc. Am. J. 81, 1537–1547.
Turner, P.A., Griffis, T.J., Lee, X., Baker, J.M., Venterea, R.T., Wood, J.D., 2015. Indirect nitrous oxide emissions from streams within the US Corn Belt scale with stream order. Proc. Natl. Acad. Sci. Unit. States Am. 112, 9839.
Velthof, G.L., Kuikman, P.J., Oenema, O., 2002. Nitrous oxide emission from soils amended with crop residues. Nutrient Cycl. Agroecosyst. 62, 249–261.
Venterea, R.T., Spokas, K.A., Baker, J.M., 2009. Accuracy and Precision Analysis of Chamber-Based Nitrous Oxide Gas Flux Estimates. Soil Sci. Soc. Am. J. 73, 1087–1093.
Voigt, C., Lamprecht, R.E., Marushchak, M.E., Lind, S.E., Novakovskiy, A., Aurela, M., Martikainen, P.J., Biasi, C., 2017. Warming of subarctic tundra increases emissions of all three important greenhouse gases — carbon dioxide, methane, and nitrous oxide. Global Change Biol. 23, 3121–3138.
Wagena, M.B., Bock, E.M., Sommerlot, A.R., Fuka, D.R., Easton, Z.M., 2017. Development of a nitrous oxide routine for the SWAT model to assess greenhouse gas emissions from agroecosystems. Environ. Model. Software 89, 131–143.
Weier, K.L., Doran, J.W., Power, J.F., Walters, D.T., 1993. Denitrification and the Dinitrogen/Nitrous Oxide Ratio as Affected by Soil Water, Available Carbon, and Nitrate. Soil Sci. Soc. Am. J. 57.
Whitfield, P.H., Bodtker, K., Cannon, A.J., 2002. Recent variations in seasonality of temperature and precipitation in Canada, 1976–95. Int. J. Climatol. 22, 1617–1644.
Yang, Q., Zhang, X., Abraha, M., Del Grosso, S., Robertson, G.P., Chen, J., 2017. Enhancing the soil and water assessment tool model for simulating N2O emissions of three agricultural systems. Ecosys. Health Sustain. 3 e01259-n/a.
Zhou, M., Zhu, B., Wang, S., Zhu, X., Vereecken, H., Brüggemann, N., 2017. Stimulation of N2O emission by manure application to agricultural soils may largely offset carbon benefits: a global meta-analysis. Global Change Biol. 23, 4068–4083.